

MAPPING OPTICALLY VARIABLE QUASARS TOWARDS THE GALACTIC PLANE

J. G. Fernandez-Trincado¹, T. Verdugo², C. Reylé¹, A. C Robin¹, J. A. de Diego³, V. Motta⁴, L. Vega⁵, J. J. Downes^{2,6}, C. Mateu^{2,6}, A. K. Vivas⁷, C. Briceño⁷, C. Abad², K. Vieira², J. Hernández², A. Nuñez⁸ and E. Gatuuz^{9,10}

Abstract. We present preliminary results of the CIDA Equatorial Variability Survey (CEVS), looking for quasar (hereafter QSO) candidates near the Galactic plane. The CEVS contains photometric data from extended and adjacent regions of the Milky Way disk (~ 500 sq. deg.). In this work 2.5 square degrees with moderately high temporal sampling in the CEVS were analyzed. The selection of QSO candidates was based on the study of intrinsic optical photometric variability of 14,719 light curves. We studied samples defined by cuts in the variability index ($V_{index} > 66.5$), periodicity index ($Q > 2$), and the distribution of these sources in the plane (A_T, γ), using a slight modification of the first-order of the structure function for the temporal sampling of the survey. Finally, 288 sources were selected as QSO candidates. The results shown in this work are a first attempt to develop a robust method to detect QSO towards the Galactic plane in the era of massive surveys such as VISTA and Gaia.

Keywords: quasar: general - surveys

1 Introduction

In the past few years the intrinsic variability of the QSO (Rengstorf et al. 2004b,a, 2006; Schmidt et al. 2010; Ross et al. 2013; Graham et al. 2014) has been used as an alternative and efficient selection method to distinguish QSO exhibiting variability from the non-variable stellar locus. Additionally, it provides unique information about the physics of the unresolved central source. This technique is free of bias in comparison with the inherent biases present in the traditional methods based in specific cuts in the color-color diagram (Hall et al. 1996; Croom et al. 2001; Richards et al. 2002; Graham et al. 2014).

The intrinsic variability of QSO has been observed in different photometric bands from UV, optical to X-ray. This intrinsic property has been proposed as an efficient method of selection (Rengstorf et al. 2006; MacLeod et al. 2012; Graham et al. 2014), and is commonly quantified using the structure function such that the amplitude of variability changes with time (Hughes et al. 1992; Collier & Peterson 2001; Bauer et al. 2009; Welsh et al. 2011). The properties of the variability in QSO have been studied in the literature and they depend on the physical properties of the source, as the presence of radio emission, timescale and others (MacLeod et al. 2012) and the large luminosity of these sources is provided by mass accretion onto super massive black holes in its

¹ Institut Utinam, CNRS UMR 6213, Université de Franche-Comté, OSU THETA Franche-Comté-Bourgogne, Observatoire de Besançon, BP 1615, 25010 Besançon Cedex, France.

² Centro de Investigaciones de Astronomía, AP 264, Mérida 5101-A, Venezuela.

³ Instituto de Astronomía, Universidad Nacional Autónoma de México, Apdo. Postal 70264, México D.F., 04510, Mexico.

⁴ Instituto de Física y Astronomía, Universidad de Valparaíso, Avda. Gran Bretaña 1111, Playa Ancha, Valparaíso 2360102, Chile.

⁵ Instituto de Astronomía Teórica y Experimental (IATE) - Córdoba, Argentina.

⁶ Instituto de Astronomía, UNAM, Ensenada, C.P. 22860, Baja California México.

⁷ Cerro Tololo Interamerican Observatory Casilla 603, La Serena, Chile.

⁸ Centro de Modelado Científico, Universidad del Zulia, Maracaibo 4001, Venezuela.

⁹ Centro de Física, Instituto Venezolano de Investigaciones Científicas (IVIC), Caracas 1040, Venezuela.

¹⁰ Escuela de Física, Facultad de Ciencias, Universidad Central de Venezuela, PO Box 20632, Caracas 1020A, Venezuela.

center (Salpeter 1964; Lynden-Bell 1969; Rees 1984).

Both methods are now used to select QSO candidates, especially in surveys with extended time coverage like the SDSS Strip 82 (MacLeod et al. 2012), MACHO (Pichara et al. 2012), Catalina Real-Time Transient Survey (Drake et al. 2009; Graham et al. 2014) and in the future with Gaia (Mignard 2012). The variability selection is a technique with a high degree of confidence (Graham et al. 2014), and recent studies have shown that variability as method for QSO selection is more accurate and has a higher degree of purity in comparison with the use of color-only cuts (Morganson et al. 2014).

Precise identification of QSOs along the Galactic plane is very valuable for astronomical reference frame purposes. The large extinction present in the area has meant that all QSO-oriented surveys have systematically avoided this region, and the scarcity of confirmed QSO there is evident. Kinematical studies of the Galactic Disk and Bulge, especially when working in small fields of view, would benefit enormously by having a dense and deep “network” on confirmed QSO, to which tie in their observations. For large-scale surveys like Gaia, it is also important to have a large enough number of QSOs identified everywhere on the sky, to improve the overall quality and spatial uniformity of the QSO reference system. Finally, the ICRF always will benefit from adding more new QSO, as the densification of their sources obviously improves the final accuracy of such fundamental reference frame.

The extensive variability survey compiled in the CIDA Equatorial Variability Survey (CEVS) since 2001 has been used so far to study a variety of topics, including RR Lyrae stars, T Tauri stars and young Brown Dwarfs, etc. (e.g. Vivas et al. 2004; Briceño et al. 2005; Downes et al. 2008; Mateu et al. 2012). At high galactic latitudes Rengstorf et al. (2004a,b, 2009) used the QUEST Variability Survey data, predecessor to the CEVS, to conduct a variability survey of QSOs over ~ 190 sq. deg. However, the CEVS has not been applied to extragalactic studies so far, particularly in the search for QSOs.

This paper is organized as follow. In §2 we briefly present the data. The methods are described in §3. The expected contamination is discussed in §4. In §5 we present a preliminar conclusion of this research.

2 Data

The CEVS provides optical multi-epoch information in the V , R and I_c photometric bands. For our work we have combined data from the QUEST* high-galactic latitude survey data, obtained during 1998 to 2001, with the CEVS data collected from 2001 to 2008. The full catalog contains more than 6.5×10^6 sources, observed multiple times from 1998 to 2008. All observations were obtained with the QUEST mosaic camera (16 CCDs) installed at the 1.0/1.5m Jürgen Stock Schmidt telescope located at the National Astronomical Observatory of Venezuela. The survey has been scanned 476 deg^2 of the sky during ten years in a region defined between $60^\circ \leq \alpha \leq 140^\circ$ and $-6^\circ \leq \delta \leq 6^\circ$ around the Galactic plane. A detailed description of the survey is given in Mateu et al. (2012).

We selected one specific section of the catalog (with a large number of observations in each band, $N > 10$), restricted to the range $85^\circ \leq \alpha \leq 87.5^\circ$ and $-1.5^\circ \leq \delta \leq -0.5^\circ$, with 14,719 sources covering an area of 2.5 deg^2 near the Galactic plane that also has with observations over 1.96 deg^2 from the SDSS DR9 (Ahn et al. 2012). This region in the CEVS has typically about 30 observations per source.

3 Selection criteria

In subsections 3.1, 3.2 and 3.3 below, we describe three methods (modified in this work), proposed in the literature to explore the intrinsic optical variability, periodicity, and the first-order of the structure function, with the main goal to separate variable QSO and point sources of non-variability sources (more likely associated with the stellar locus).

*Quasar Equatorial Survey Team

3.1 Variability

We adopted a formulation to that of eq. 1 in Rengstorf et al. (2006), in order to characterize the variability over three optical photometric bands, V , R and I_c of the CEVS. For this purpose, we defined the index of variability V_{index} according to the following criteria: (i) A minimum of 10 observations was imposed in each photometric band; (ii) The index $P(\chi^2)$ given by the CEVS, represents the probability of variability for each photometric band, and its value is related to the χ^2 (e.g., Vivas et al. 2004). The V_{index} of a star is redefined in this work as:

$$V_{index} \equiv \sum_{j=1}^3 \frac{(N^j/N_T^j) \times (1 - P(\chi_j^2)) \times 100}{\sum_{j=1}^3 (N^j/N_T^j)} = V^{j=1} + V^{j=2} + V^{j=3}, \quad (3.1)$$

where j indexes over filters ($j = 1$ for V , $j = 2$ for R , $j = 3$ for I_c); N^j is the number of observations for the i -th source and N_T^j is the maximum number of observations inside a cone search of 30 arcsec radius centered on the i -th source of the catalog. We have computed V_{index} , for 14,719 sources, and we have found for each photometric band the following percentages of sources for which $V^j \neq 0$: $V^{j=1} = 30.90\%$, $V^{j=2} = 54.77\%$ and $V^{j=3} = 65.35\%$. Figure 1 shows the cumulative probability distribution ($F > V_{index}$) for these 14,719 sources (black line) and 39 spectrally confirmed QSO (red line) from the SDSS DR9. The black vertical dashed line, correspond to the limit $V_{index} = 66.5$ imposed in this work to separate non-variable sources of variable sources, which is the same value proposed by Rengstorf et al. (2006). Finally, we selected 1,931 variable sources with $V_{index} \geq 66.5$, for which the cumulative probability distribution of $F(> 66.5)$ is about 13% and $F(> 66.5) = 5\%$ for the QSO reported in this region of the sky.

3.2 Periodicity

For our pre-selection of 1,931 variable sources in §3.1, we redefined the parameter Q , in order to separate periodic from aperiodic variable sources. We analyzed each light-curve independently, considering a minimum of ten available epochs taken from 1998 to June 2008, for the temporal sampling in the light-curves. The parameter Q , was redefined in a very similar way as eq. 7 in (Rengstorf et al. 2006):

$$Q \equiv \frac{\sum_j (N^j/N_T^j) \times \left(\frac{\sum_k (N^j/N_k^j) \times (\sigma_T^j/\sigma_k^j)^2}{\sum_k (N^j/N_k^j)} \right) \times \Delta \langle m^j \rangle_{\max}}{\sum_j (N^j/N_T^j) \times \sigma_T^j}, \quad (3.2)$$

where the index j , N^j and N_T^j are defined as in the previous subsection; the index k correspond to the number of 15-days intervals within the time series of observations of the star; N_k and σ_k correspond to the number of observations in each bin and the standard deviation of the magnitudes by bin in the light curve, respectively; σ_T correspond to the total standard deviation of the magnitudes. Figure 1 shows the Q distribution for our pre-selected 1,931 variable sources. We found 1,481 sources, and 2 spectrally confirmed QSO from SDSS DR9, satisfying the condition of aperiodicity, that is $Q > 2$, based in previous studies (Rengstorf et al. 2006), set to minimize contamination by likely periodic variables.

3.3 First-order of the structure function

So far, we have done a pre-selection of 1,481 sources identified as potential variable and aperiodic QSO in the CEVS. Our final step, consist in identifying the location of QSO candidates in the plane (A_T, γ_T) . The first-order of the structure function, which quantify the variability amplitude as a function of time, has been used used for this purpose. We computed an equivalent formulation, rewriting Eq. 3 in Schmidt et al. (2010):

$$M_{i,l}(\Delta t_{i,l}) \equiv \left\langle \sqrt{\frac{\pi}{2}} |\Delta m_{i,l}| - \sqrt{\sigma_i^2 + \sigma_l^2} \right\rangle_{\Delta t}, \quad (3.3)$$

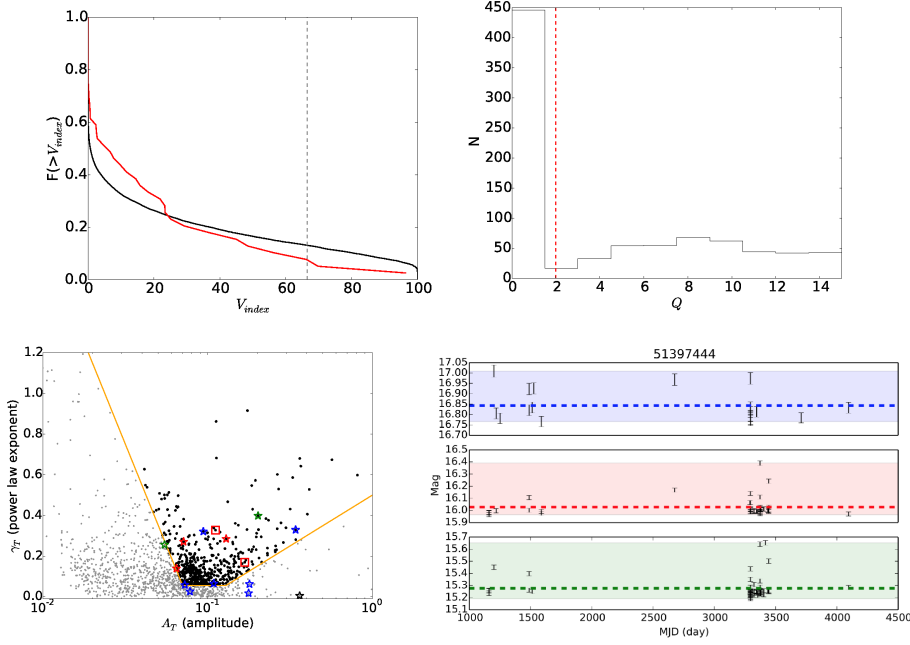


Fig. 1. Top left panel: Cumulative probability distribution ($F > V_{index}$) for 14,719 sources from the CEVS (black line), and QSO spectrally confirmed in the SDSS DR9 (red line) and observed by CEVS. The vertical dashed line corresponds to the limit used in this work ($V_{index} = 66.5$), to rejected non-variable sources ($V_{index} < 66.5$). **Top right panel:** Q_i distributions for 1,931 variable sources. QSOs candidates have $Q > 2$, meaning that they are both variable and aperiodic sources. **Bottom left panel:** QSO candidates parametrized by the structure function in the plane (A_T, γ_T) are shown with black dots and QSO spectrally confirmed are shown in red open squares. All dots correspond to the sample of 1,481 sources analyzed in the third step (see § 3.3). Contaminants in our sample reported in the literature are: binary stars (blue open stars), RR Lyrae (black open star), brown dwarfs (green open stars), variable stars in the CATALINA survey (open red stars). **Bottom right panel:** Example of a QSO candidate light-curve. From top to bottom observations in the photometric bands V , R and I_c respectively, are shown.

where $\Delta m_{i,l}$ is the measured magnitude difference between observation i and l , and σ_i and σ_l are the photometric errors, being $\Delta t_{i,l}$ the time difference between two observations. Thus, the average is taken over all epoch pairs i, l that falls in the bin Δt . In the same way as Schmidt et al. (2010), we parametrized the structure function as:

$$M_{i,l}^{mod}(\Delta t_{i,l} | A^j, \gamma^j) \equiv A^j \left(\frac{\Delta t_{i,l}}{1\text{yr}} \right)^{\gamma^j}, \quad (3.4)$$

where the subindex j stands for filter, and can take the values, V, R, I, and:

$$A_T = \frac{\sum_j \left(N^j / N_T^j \right) \times A_j}{\sum_j \left(N^j / N_T^j \right)}, \quad (3.5)$$

and

$$\gamma_T = \frac{\sum_j \left(N^j / N_T^j \right) \times \gamma_j}{\sum_j \left(N^j / N_T^j \right)^j}, \quad (3.6)$$

Figure 1 show the distribution A_T and γ_T for the pre-selected 1,481 sources, and the best fitting values of Eq. (3.4) to Eq. (3.6) to the data. We defined a QSO selection box as Eq. 7 to Eq. 9 in Schmidt et al. (2010),

which led us to select a sample of 288 QSO candidates.

The final sample of candidates is shown in the Table 1, containing all the relevant information for each star in it: column 1-10 list ID (CEVS-QSO-XXX; notation adopted in this work), mean V , R and I_c magnitudes, number of times each star was observed in each photometric band and amplitude. The index of variability and aperiodicity are presented in columns 11 and 12 respectively, and column 13 and 14, correspond to the parameters of the structure function (A_T and γ , respectively). Table 1 is published in its entirety in a public repository^{†‡}. A sample of the table is shown here for guidance regarding its content.

Table 1. Photometric parameters of QSO candidates from the CIDA Equatorial Variability Survey (CEVS).

| ID | $\langle V \rangle$ [mag] | $\langle R \rangle$ [mag] | $\langle I \rangle$ [mag] | Nv | Nr | Ni | AmpV [mag] | AmpR [mag] | AmpI [mag] | Vindex | Q | A_T | γ_T |
|--------------|------------------------------|------------------------------|------------------------------|----|----|----|---------------|---------------|---------------|--------|----------|-------|------------|
| CEVS-QSO-001 | 19.323 | 18.045 | 17.855 | 11 | 41 | 79 | 1.009 | 1.019 | 0.951 | 100.00 | 58.671 | 0.109 | 0.285 |
| CEVS-QSO-002 | 19.449 | 19.010 | 18.299 | 18 | 43 | 70 | 0.566 | 0.412 | 0.696 | 99.99 | 59.737 | 0.068 | 0.253 |
| CEVS-QSO-003 | 19.371 | 18.791 | 18.037 | 16 | 47 | 91 | 0.875 | 0.670 | 0.897 | 100.00 | 115.831 | 0.088 | 0.232 |
| CEVS-QSO-004 | 19.438 | 18.699 | 17.644 | 9 | 45 | 87 | 1.072 | 0.584 | 0.591 | 100.00 | 124.065 | 0.066 | 0.126 |
| CEVS-QSO-005 | 18.747 | 18.450 | 17.170 | 17 | 49 | 99 | 0.947 | 0.493 | 0.319 | 73.36 | 1243.269 | 0.049 | 0.425 |
| CEVS-QSO-006 | 19.182 | 17.886 | 16.372 | 26 | 52 | 90 | 0.455 | 0.454 | 0.357 | 100.00 | 986.204 | 0.341 | 0.329 |
| CEVS-QSO-007 | 19.505 | 18.916 | 18.172 | 3 | 32 | 36 | 0.431 | 0.508 | 0.517 | 99.72 | 28.757 | 0.115 | 0.071 |
| CEVS-QSO-008 | 18.999 | 18.545 | 17.540 | 30 | 50 | 78 | 0.703 | 1.012 | 0.607 | 91.33 | 54.579 | 0.062 | 0.346 |
| CEVS-QSO-009 | 19.632 | 18.743 | 17.851 | 14 | 43 | 69 | 0.563 | 0.569 | 0.561 | 99.99 | 6.741 | 0.132 | 0.467 |

4 Expected Milky Way contamination

We have compared the synthetic colour-magnitude diagram computed with the Besançon galaxy model (hereafter BGM) (Robin et al. 2003, 2014), for the same line-of-sight and solid angle studied in this paper. The simulation was generated taking the selection function of the data into account. Since we are near the Galactic plane, we expect a high degree of contamination (foreground stars), not present in previous surveys of QSO using variability. The absence of a complete catalog of confirmed QSOs in this part of the Galaxy makes it difficult to estimate such contamination, a key point to validate our methodology and its application in future surveys like Gaia or VISTA. At this moment we are in the process of determining this contamination, since the CEVS is a not homogeneous survey. However we can do a simple and rough estimate of the more likely contaminants in our sample, namely K and M-type stars, using the BGM and comparing the synthetic colors with those observed in our sample candidates (see Figure 2).

5 Conclusion

In this work, we have used the multiepoch data in the large scale CEVS to search for low-galactic latitude QSOs by their intrinsic optical variability, using an alternative formulation similar to the proposed in the literature, in order to detect QSO candidates from inhomogeneous temporal sampling.

We have selected 288 QSO candidates according to their variability, aperiodicity and parameters of the structure function, over an area of 2.5 deg^2 . Extrapolating these results to the full CEVS with an total area of $\sim 500 \text{ deg}^2$, we estimate that is possible to detect 52,000 new QSO candidates in this survey. However, we have shown that the methods presented in this work are sensitive to variations in the temporal sampling of the light curves. This explains the fact our method rejects 95% of the QSO spectroscopically confirmed in the region in common with the SDSS DR9 survey. Follow-up spectroscopic observations for our QSO candidates are currently conducted at the REOSC Spectrograph installed on the 2.15-m telescope at CASLEO, Argentina.

[†]<http://fernandez-trincado.github.io/Fernandez-Trincado/simulations.html>

[‡]fernandez@obs-besancon.fr

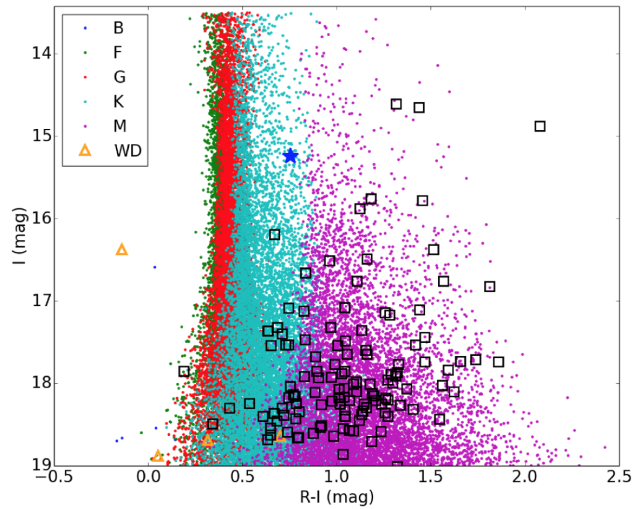


Fig. 2. Color magnitude diagram for QSO candidates (black symbols) with I and R information. The blue star refers to object ID 51397444 showed in Figure 1. The simulation of the Besançon galaxy model is presented with dots of different colors for each stellar population, which are labelled by spectral type (B, F, G, K, M and white dwarfs WD).

In the near future, large spectroscopic surveys as Gaia may help to confirm QSO sources, selected from variability surveys towards the Galactic plane, allowing us to quantify the selection efficiency.

J.G.F-T is currently supported by Centre National d'Etudes Spatiales (CNES) through Ph.D grant 0101973 and the Région de Franche-Comté, and by the French Programme National de Cosmologie et Galaxies (PNCG). This research was supported by the Munich Institute for Astro- and Particle Physics (MIAPP) of the DFG cluster of excellence "Origin and Structure of the Universe". V.M. acknowledges the support from FONDECYT 1120741, and Centro de Astrofisica de Valparaiso.

References

- Ahn, C. P., Alexandroff, R., Allende Prieto, C., et al. 2012, *ApJS*, 203, 21
 Bauer, A., Baltay, C., Coppi, P., et al. 2009, *ApJ*, 696, 1241
 Briceño, C., Calvet, N., Hernández, J., et al. 2005, *AJ*, 129, 907
 Collier, S. & Peterson, B. M. 2001, *ApJ*, 555, 775
 Croom, S. M., Smith, R. J., Boyle, B. J., et al. 2001, *MNRAS*, 322, L29
 Downes, J. J., Briceño, C., Hernández, J., et al. 2008, *AJ*, 136, 51
 Drake, A. J., Djorgovski, S. G., Mahabal, A., et al. 2009, *ApJ*, 696, 870
 Graham, M. J., Djorgovski, S. G., Drake, A. J., et al. 2014, *MNRAS*, 439, 703
 Hall, P. B., Osmer, P. S., Green, R. F., Porter, A. C., & Warren, S. J. 1996, *ApJ*, 462, 614
 Hughes, P. A., Aller, H. D., & Aller, M. F. 1992, *ApJ*, 396, 469
 Lynden-Bell, D. 1969, *Nature*, 223, 690
 MacLeod, C. L., Ivezić, Ž., Sesar, B., et al. 2012, *ApJ*, 753, 106
 Mateu, C., Vivas, A. K., Downes, J. J., et al. 2012, *MNRAS*, 427, 3374
 Mignard, F. 2012, *Mem. Soc. Astron. Italiana*, 83, 918
 Morganson, E., Burgett, W. S., Chambers, K. C., et al. 2014, *ApJ*, 784, 92
 Pichara, K., Protopapas, P., Kim, D.-W., Marquette, J.-B., & Tisserand, P. 2012, *MNRAS*, 427, 1284
 Rees, M. J. 1984, *ARA&A*, 22, 471
 Rengstorf, A. W., Brunner, R. J., & Wilhite, B. C. 2006, *AJ*, 131, 1923
 Rengstorf, A. W., Mufson, S. L., Abad, C., et al. 2004a, *ApJ*, 606, 741
 Rengstorf, A. W., Mufson, S. L., Andrews, P., et al. 2004b, *ApJ*, 617, 184
 Rengstorf, A. W., Thompson, D. L., Mufson, S. L., et al. 2009, *ApJS*, 181, 129

- Richards, G. T., Fan, X., Newberg, H. J., et al. 2002, *AJ*, 123, 2945
- Robin, A. C., Reylé, C., Derrière, S., & Picaud, S. 2003, *A&A*, 409, 523
- Robin, A. C., Reylé, C., Fliri, J., et al. 2014, *A&A*, 569, A13
- Ross, N. P., McGreer, I. D., White, M., et al. 2013, *ApJ*, 773, 14
- Salpeter, E. E. 1964, *ApJ*, 140, 796
- Schmidt, K. B., Marshall, P. J., Rix, H.-W., et al. 2010, *ApJ*, 714, 1194
- Vivas, A. K., Zinn, R., Abad, C., et al. 2004, *AJ*, 127, 1158
- Welsh, B. Y., Wheatley, J. M., & Neil, J. D. 2011, *A&A*, 527, A15